

Dedham, MA: Artech 1981.

[15]. V. A. Monaco, and P. Tiberio, "Automatic Scattering Matrix Computation of Microwave Circuits,"

Vol. 39, 1970. pp. 59-64.

[16]. N. Kuhn, "Simplified Signal Flow Graph Analysis," *Microwave J.*, 1963, VI, No. 11., pp. 59-66.

[17]. F. L. Warner, Microwave Attenuation Measurement, Peter Peregrinus, 1977. pp. 276.

[18]. H. Liao and W. Dai, "Wave Spreading Evaluation of Interconnect Systems," University of California Technical Report, UCSC-CRL-92-40, Sept. 1992.

## 7. References

- [1]. J. Dobrowolski, Introduction to Computer Methods for Microwave Circuit Analysis and Design, Artech House, 1991.
- [2]. P. O'Brien, T. Savarino, "Modeling the Driving -Point Characteristic of Resistive Interconnect for Accurate Delay Estimation," Digest of Technical Papers, ICCAD-89, Santa Clara, pp. 512-515.
- [3]. J. Robinstein, P. Penfield, and M. Horowitz, "Signal Delay in RC Tree Networks," *IEEE Trans. On CAD*, Vol. CAD-2, no. 3, July 1983, pp. 202-211.
- [4]. T. Lin, C. Mead, "Signal Delay in General RC networks," *IEEE Trans. on CAD*, Vol. CAD-3, no. 4, Oct. 1984, pp. 331-349.
- [5]. P. Chan, K. Karplus, "Computing Signal Delay in General RC Networks by Tree/Link Partitioning," 26th ACM/IEEE Design Automation Conference Proceedings, 1989, pp. 485-490.
- [6]. P. Chan, M. Schlag, "Bounds on Signal Delay in RC Mesh Networks," *IEEE Trans. on CAD*, Vol. CAD-8, no. 6, June 1989. pp. 581-589
- [7]. R. Rohrer, "Circuit Partitioning Simplified," *IEEE. Trans. on CAS*, Vol. 35, no. 1, Jan. 1988. pp. 2-5.
- [8]. W. C. Elmore, "The Transient Response of Damped Linear Networks with Particular Regard to Wideband Amplifier," *J. Applied Physics*, 19(1), 1948.
- [9]. L. T. Pillage, and R. A. Rohrer, "Asymptotic Waveform Evaluation for Timing Analysis," *IEEE Trans. on CAD*, Sept. 1990.
- [10]. L. T. Pillage, X. Huang, and R. A. Rohrer, "Asymptotic Waveform Evaluation for Circuits Containing Floating Nodes," *1990 IEEE International Symposium on Circuits and Systems*, New Orleans, LA. pp.613-616.
- [11]. C. Ratzlaff, N. Gopal, and L. Pillage, "RICE: Rapid Interconnect Circuit Evaluator," *28th ACM/IEEE Design Automation Conference Proceedings*, 1991. pp. 555-560.
- [12]. F. Y. Chang, "Waveform Relaxation Analysis of RLGC Transmission Lines," *IEEE Trans. on Circuits and Systems*, Vol. CAS-37, pp. 1394-1415, Nov. 1990.
- [13]. P. A. Rizzi, Microwave Engineering, Englewood Cliffs, NJ. Prentice-Hall, 1988.
- [14]. K. C. Gupta, R. Grag, and R. Chadha, Computer Aided Design of Microwave Circuits,

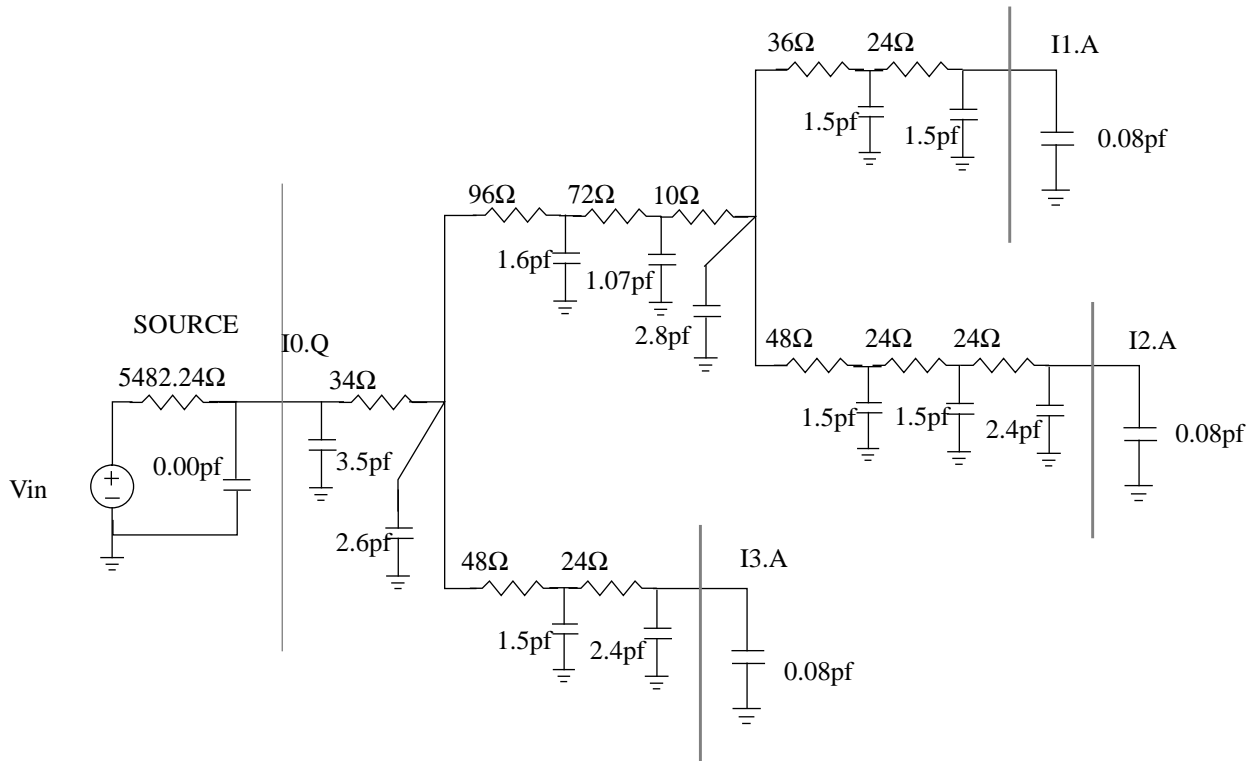


Figure 9. An RC tree network used for delay computation.

**Table 1: Delay result comparison**

	$\pi$ model	macromodel	SPICE	$\pi$ model ERROR	macromodel ERROR
I0.Q to I1.A	3.242ns	3.239 ns	3.233 ns	0.28%	0.19%
I0.Q to I2.A	3.518ns	3.508 ns	3.508 ns	0.30%	0.0%
I0.Q to I3.A	0.954ns	0.962 ns	0.958	0.42%	0.42%

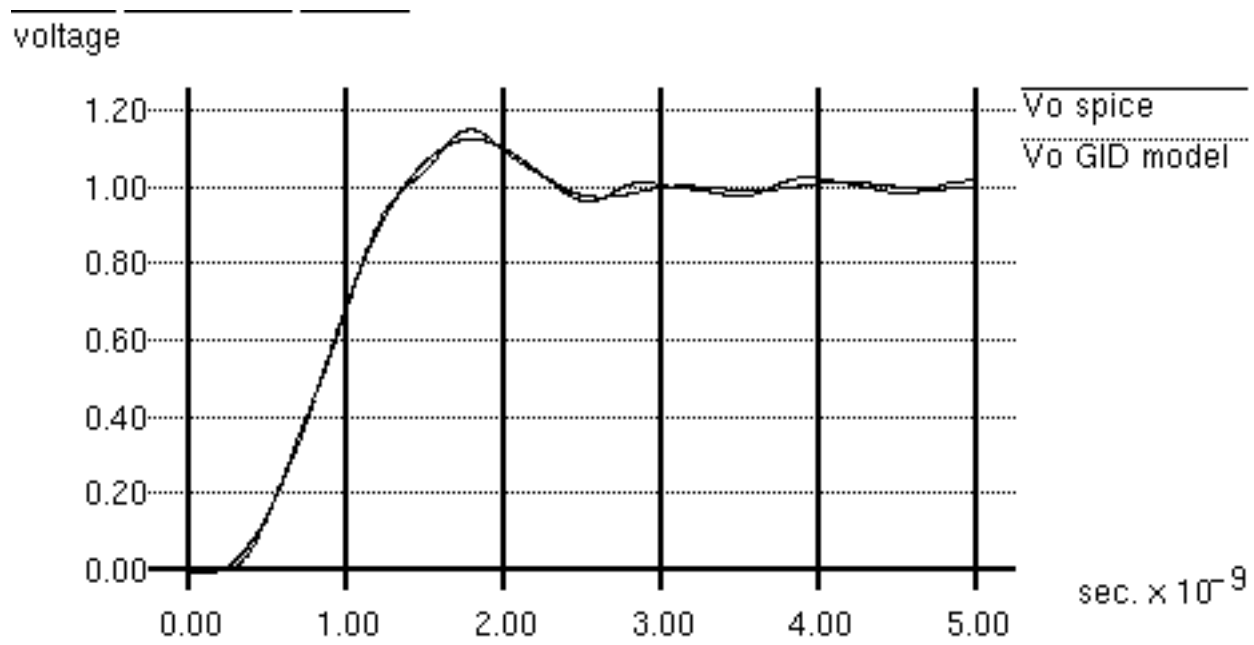


Figure 7c. Far-end voltage response vo.

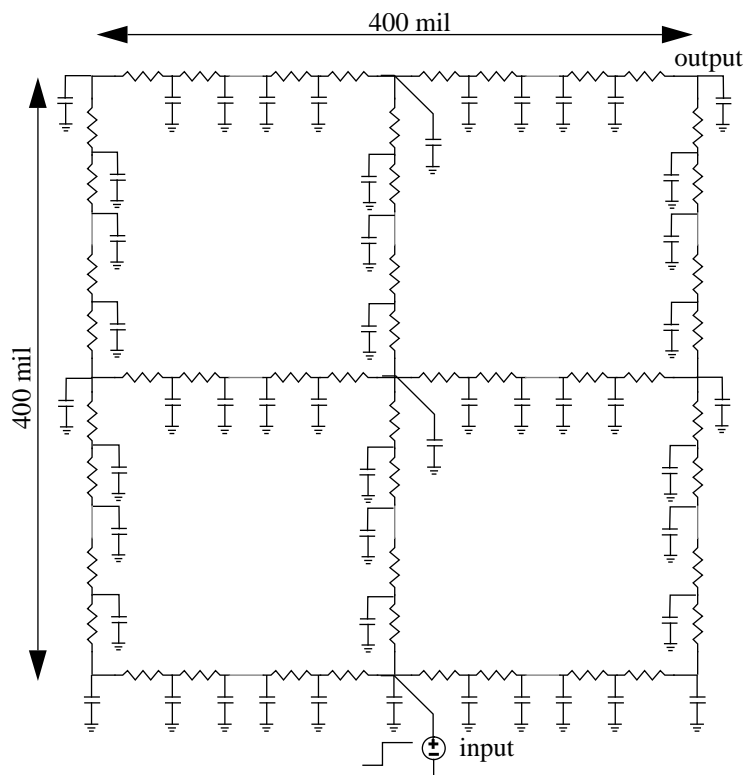


Figure 8. A grid-type clock network.

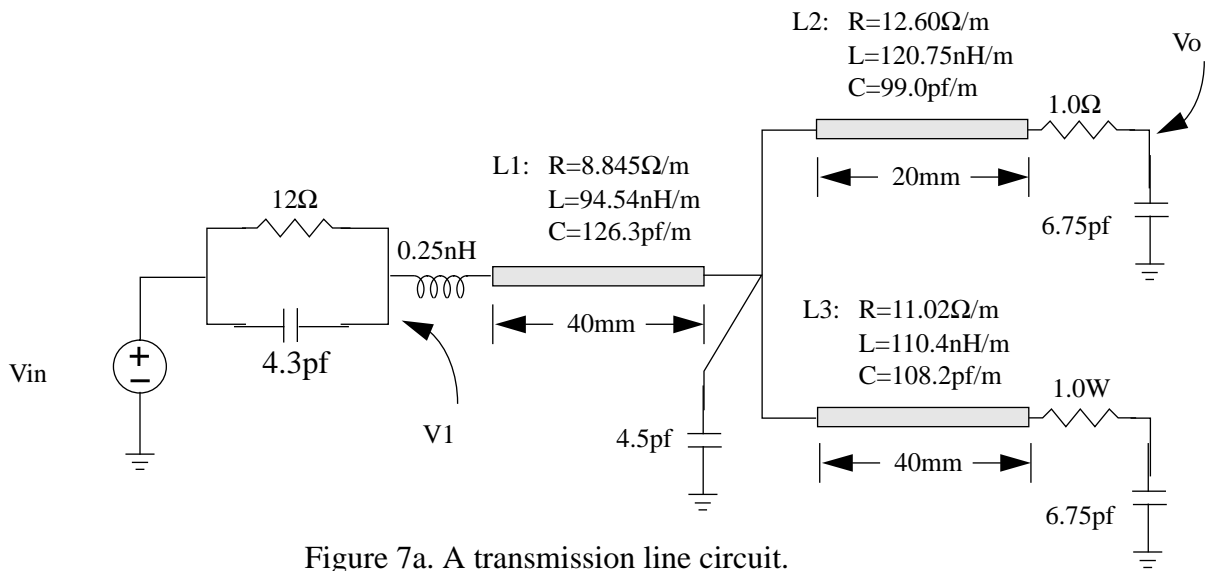


Figure 7a. A transmission line circuit.

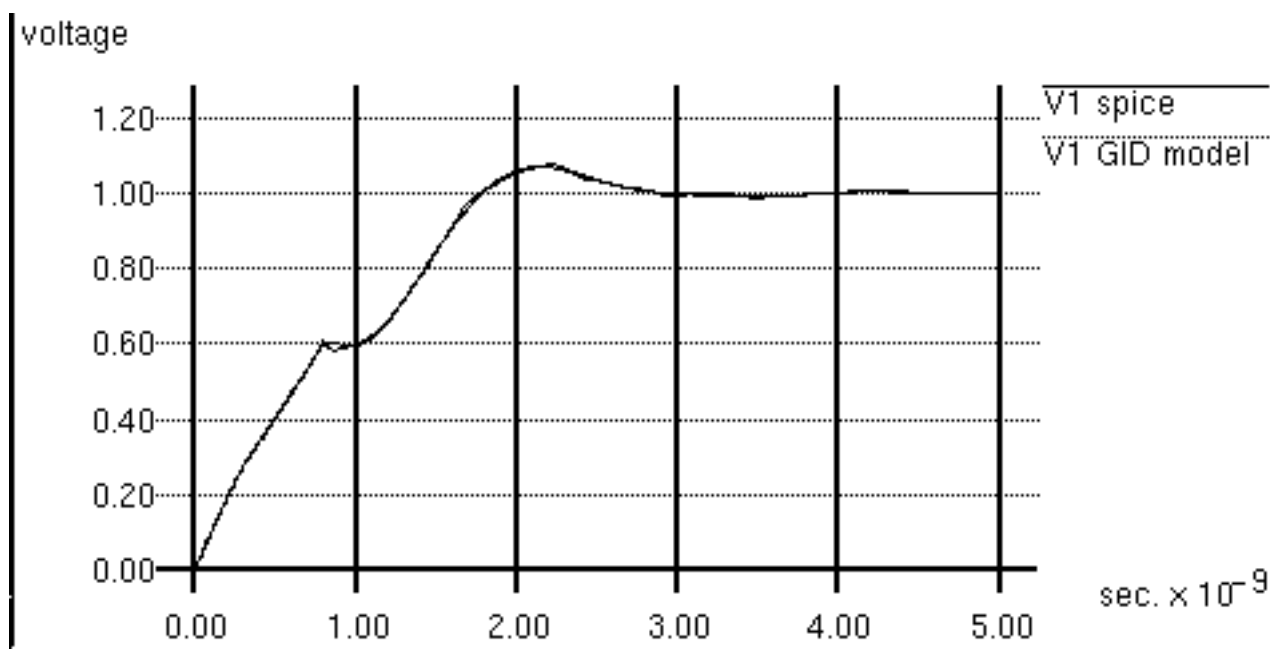


Figure 7b. Near end voltage response v1.

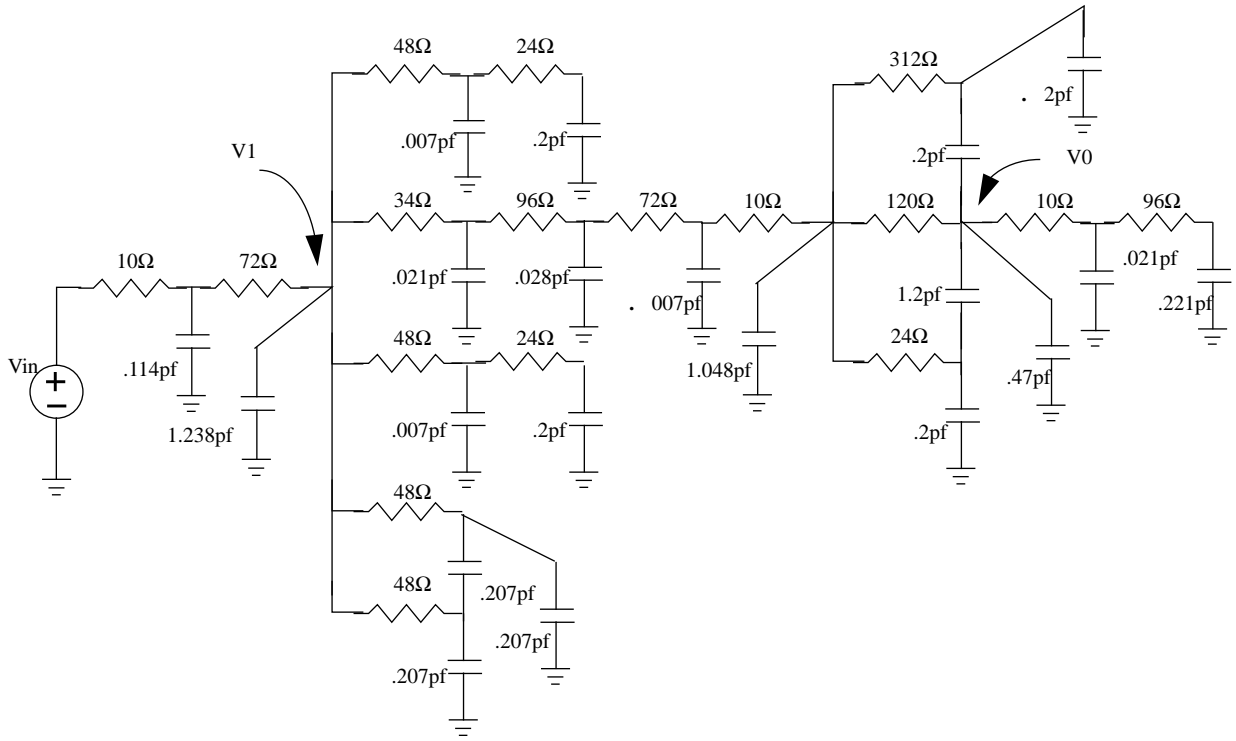


Figure 6a. A RC circuit with floating capacitance loops.

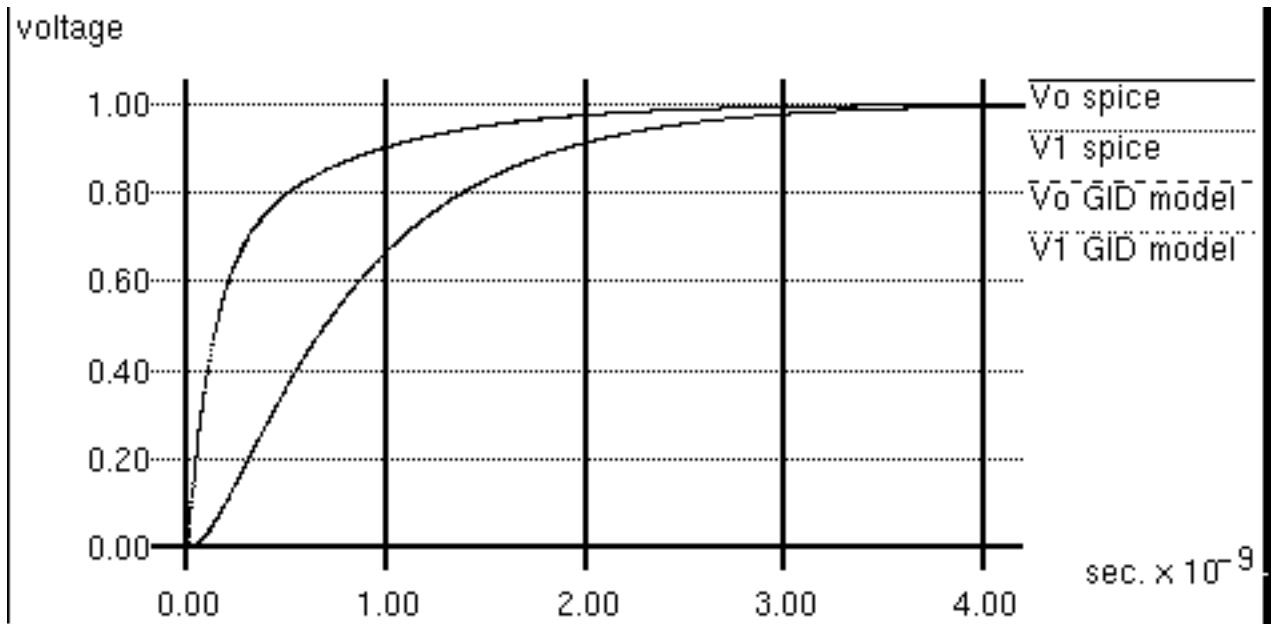


Figure 6b. Output response v1 and vo.

the distributed representation of the interconnect and by the fact that only the external nodes need to be analyzed.

In the last example shown in Figure (9), we made comparisons of delay computation using the macromodel to both SPICE and the Driving-Point Admittance Approximation, also known as  $\pi$  model introduced in [2]. We have chosen an RC tree since this is the only structure to which  $\pi$  model can be applied. The results of delay computations using the  $\pi$  model in [2], SPICE, and macromodel are given in Table 1. The macromodel uses 2<sup>nd</sup> order approximation in the example. Due to the simple RC tree structure, both the  $\pi$  model and the macromodel result in very accurate delays. However, the  $\pi$  model does not have the flexibility to extend the computation to general mesh networks and distributed transmission line networks. Moreover, the order of approximation in the  $\pi$  model is not adjustable for more complicated circuits.

## 6. Conclusion

We have developed a S-Parameters based macromodel of distributed-lumped networks. The macromodel is versatile such that networks with capacitive cutsets, inductive loops, and lossy transmission lines can be easily handled. To improve the efficiency of the simulation, the Adjoined Merging Rule and the Self Merging Rule are derived to reduce the original network into a network containing a multiport with the sources and loads of interest. The S-Parameters of the circuit components are approximated by Taylor series to simplify the reduction process. Pade approximation is then applied to the reduced network to obtain the macromodel. The macromodel is very flexible that the accuracy of the model can be controlled by adjusting the order of approximation, so that at different design stages, the simulation accuracy and speed are combined to determine the level of the macromodel needed. The macromodel has been used for the transient analysis of lumped and distributed networks and the experimental results indicate that our model can approach the accuracy of SPICE with one or two order less computing time.

the system. Special considerations to the approximation method for the analysis of the particular type of systems presented in this paper will be included in the full submission.

## 5. Experimental results

Several benchmark examples are used to verify the efficiency and generality of the macromodel. These testing circuits include various topologies commonly encountered in the delay modeling of VLSI interconnects. All benchmarks were executed on a Sun Sparc 1+ station.

The first circuit, shown in Figure (6a), is a RC network. Floating capacitors are present to form several loops. It took 0.2 CPU second to analyze the circuit with one external output node and 0.3 CPU second for two external output nodes, both using second order macromodel. The output responses with a unit step input, together with the results obtained by SPICE2G6, are plotted in Figure (6b). While there is little difference between the results based on macromodel and the SPICE model, it took SPICE2G.6 3.2 CPU second to compute the response.

The second testing circuit consists of three lossy transmission lines, a floating capacitor and an inductor. (See Figure 7a). Only 0.2 CPU second is used to analyze the circuit from the source to two output nodes. On the other hand, 41.7 CPU second is needed for SPICE2G.6 to analyze this circuit where L1 and L3 are represented by 30 lumped sections, and L2 by 15 lumped sections. The input signal has a 0.8ns rise time, and the results are shown in Figure (7b) and (7c).

A grid-type clock network, (see Figure (8)), first given in [11] for the RICE simulator is also analyzed using the macromodel. The clock is distributed around the periphery of a 400mil x 400mil chip. The vertical runs are on metal 1 ( $R=80\Omega/100\text{mil}$  and  $C=0.5\text{pf}/100\text{mil}$ ) and the horizontal runs are on metal 2 ( $R=160\Omega/100\text{mil}$  and  $C=0.4\text{pf}/100\text{mil}$ ). Represented by lumped RC elements, it contains 12001 nodes and 24001 branches. It took 2,206 seconds for AWESim[9] to analyze the circuit. RICE[11] used 4.96 CPU second on Sun Sparc 1 station to read and parse the circuit descriptions due to the fact that transmission lines are represented by a lot of lumped sections, another 0.81 second to perform the computation. On the other hand, our program took 0.2 second CPU time for the analysis from the source to one output node and 0.9 second is need for the analysis from source to all other 8 nodes. The computation time is significantly reduced by



computation. The two port network under discussion is shown in Figure 5.

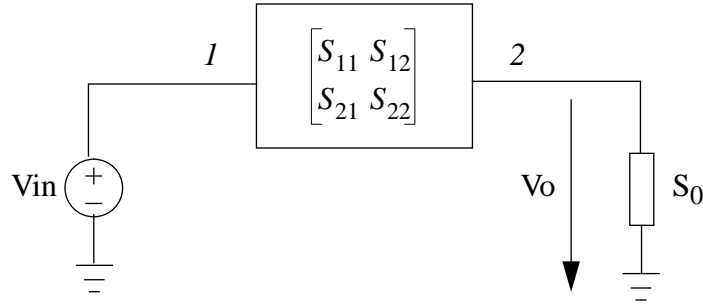


Figure 5. A two port network.

Recall the scattering matrix definition [1], for a linear n-port system with incident wave  $A = [a_1, a_2, \dots, a_n]^T$  and reflected wave  $B = [b_1, b_2, \dots, b_n]^T$ , we have:

$$B = SA \quad (11)$$

Define the voltage and current vectors for the system to be:

$$V = A + B, \quad I = Z_c^{-1} \times (A - B) \quad (12)$$

where  $Z_c$  is the diagonal reference impedance matrix.

For the two-port system shown in Figure 5, we have the following voltage transfer function in the frequency domain:

$$H(s) = \frac{S_{21} (1 + S_0)}{1 + S_{11} + S_0 (S_{12} S_{21} - S_{11} S_{22} - S_{22})} \quad (13)$$

Once the transfer function is obtained, the Pade approximation method [9] can be used to analyze

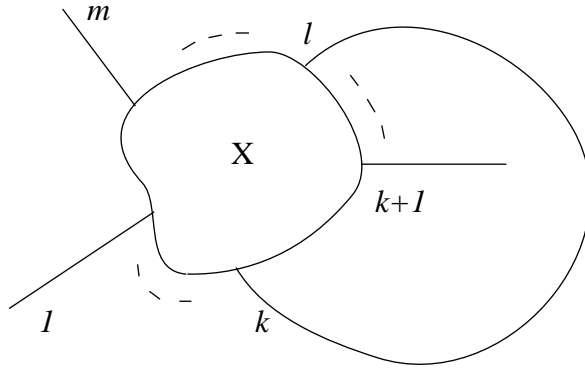


Figure 4. Self Merging.

The derivation of the two reduction rules will be presented in the final paper. Given an arbitrary distributed-lumped network  $L$  described by the linear components discussed in section 2, let  $E_n$  be the set of external  $n$  nodes. The network reduction process begins with merging all internal components by repeatedly utilizing the Adjoined Merging rule for all the nodes  $i$  that does not belong to  $E_n$ . The Self Merging rule is applied to eliminate all the self loops introduced by the Adjoined Merging process. Finally, an  $n$ -port network characterized by its scattering parameters is derived. Notice that the S-Parameters are approximated by their lower order moments.

It should be pointed out that the above reduction process does not require the network be an RC tree. Since we start with the S-Parameter description of the system, which always exists for any physically realizable system, the formulation is completely general for any linear distributed-lumped network with analytical component descriptions. Another advantage is that the need for using lumped representation of transmission lines is eliminated since lossy transmission lines can be represented in the distributed form.

#### 4. S-Parameter based macromodel

Without loss of generality, assume a two port network is the result of the network reduction process (see Figure 5). In this section, we develop the macromodel for delay and timing

$(n + m - 2) \times (n + m - 2)$  port system has the following S-parameters:

$$S_{ji} = \begin{cases} Sx_{ji} + \frac{Sx_{ki}Sy_{ll}Sx_{jk}}{1 - Sx_{kk}Sy_{ll}} & i, j \in X \\ \frac{Sx_{ki}Sy_{jl}}{1 - Sx_{kk}Sy_{ll}} & i \in X, j \in Y \end{cases} \quad (9)$$

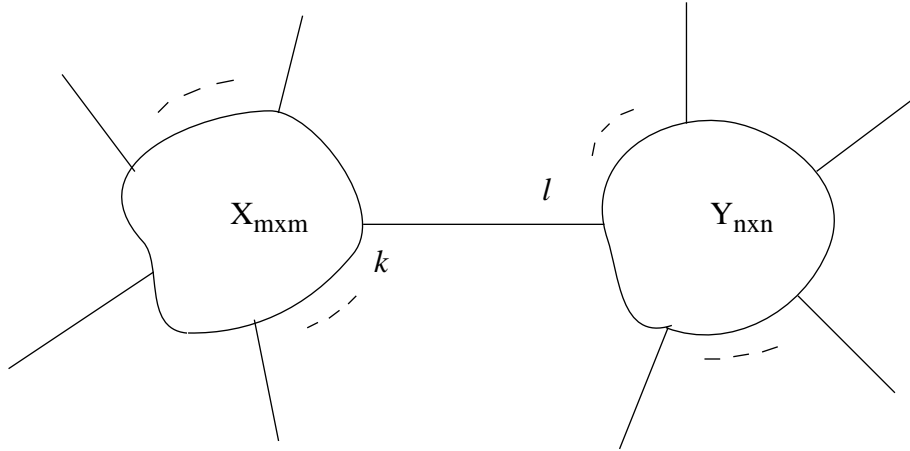


Figure 3. Adjoined Merging.

### Self Merging Rule:

Let  $X$  be an  $m$  port system with a self loop connected to the  $l^{\text{th}}$  and  $k^{\text{th}}$  ports in  $X$  (see Figure 4). After eliminating the self loop, the resultant  $(m - 2)$  port system has the following S-parameters:

$$S_{ji} = Sx_{ji} + Sx_{jl}a_l + Sx_{jk}a_k \quad i, j = 1, 2, \dots, m - 2 \quad (10)$$

where

$$a_l = \frac{1}{\Delta} (Sx_{li}Sx_{kk} + Sx_{ki}(1 - Sx_{lk}))$$

$$a_k = \frac{1}{\Delta} (Sx_{ki}Sx_{ll} + Sx_{li}(1 - Sx_{kl}))$$

$$\Delta = (1 - Sx_{lk})(1 - Sx_{kl}) - Sx_{ll}Sx_{kk}$$

The network reduction problem can be defined as follows: given a linear distributed-lumped

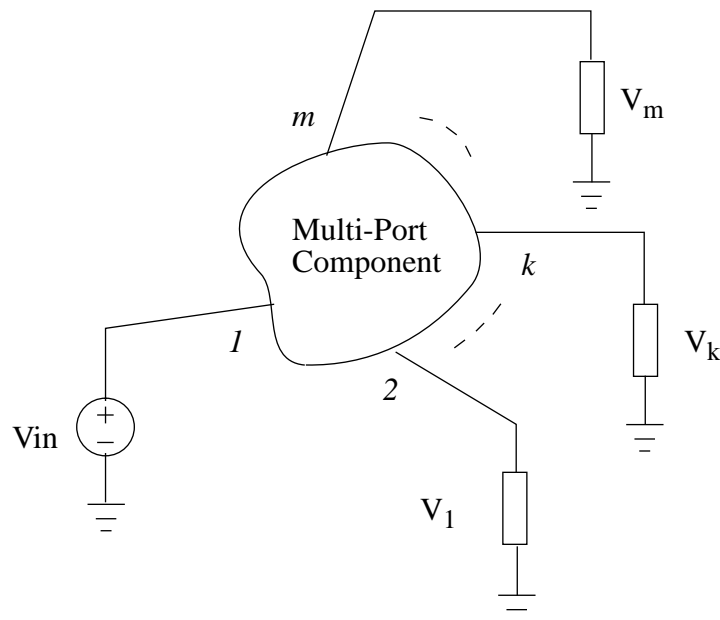


Figure 2. A multiport representation.

network consisting of the elements defined in Figure (1a) through (1d), find a multiport representation of the network as illustrated by Figure 2, where the multiport is characterized by its S-parameters. All nodes in the network are internal to the multiport except the node connected to the driving source (node 1) and the loads of interest (nodes 2 through  $m$ ). These external nodes are specified by the user.

To obtain such a multiport representation with  $m$  external ports from an arbitrary distributed-lumped network of  $n$  original nodes, the network is reduced by merging the nodes into the multiport one at a time while keeping all user specified nodes external. There are two basic reduction rules:

**Adjoined Merging Rule:**

Let  $X$  and  $Y$  be two adjoined multiports, with  $m$  ports and  $n$  ports respectively. Assume port  $k$  of  $X$  is connected to port  $l$  of  $Y$ , as shown in Figure 3. After merging  $X$  and  $Y$ , the resultant

Then, a *Multiplication Operation* is defined as:

$$C = A \times B = \sum_{i=0}^n c_i s^i \quad \text{with} \quad c_i = \sum_{j=0}^i a_j b_{i-j} \quad (7)$$

And a *Division Operation*:

$$D = A/B = \sum_{i=0}^n d_i s^i \quad \text{with} \quad d_i = \frac{1}{b_0} \left( a_i - \sum_{j=0}^{i-1} d_j b_{i-j} \right) \quad (8)$$

From (8) it seems that a negative first moment  $d_{-1}$  would be created if  $b_0 = 0$ . However, since we use Scattering Parameters to characterize all components, all Scattering Parameters of passive components have no poles at  $s = 0$  based on the principle of energy conservation[13]. Therefore, if  $D$  represents an element of a scattering matrix, it is guaranteed that there is no pole at  $s = 0$ . This implies that if  $b_0 = 0$ ,  $a_0$  must be zero, so we can shift all moments of  $A$  and  $B$  to the left and keep  $b_0 \neq 0$ .

### 3. Network reduction algorithm

Given the individual component scattering parameters presented in the last section, we are ready to describe a systematic reduction algorithm to reduce a distributed-lumped network to a multiport with sources and loads of interest.

Several network reduction algorithms have been reported. The multiport connection method was introduced in [1, 14, 15]. In this method, the Scattering-matrix of the network is partitioned into blocks based on classification of internal and external ports. The Scattering-Matrix can be obtained using block operations including time-consuming matrix inversion. Connecting two multiports at a time from bottom up may reduce the computation time. However, matrix inversion is still unavoidable. Kuhn [16] introduced a flow graph reduction method. A microwave network is represented by a flow graph and the graph can be reduced step-by-step based on four reduction rules. In this paper, we introduce two simple rules for fast network reduction. While Kuhn reduces the network one branch at a time, we reduce the network one node at a time. Unlike the previous approaches, our method approximates S-parameter by expanding them into Taylor series, which further improves the efficiency of our reduction process. In a later section, we will show the approximation is accurate for delay computation.

around  $s = 0$ . Note that for Equation (3) we have:

$$\cosh (\gamma) = \sum_{i=0}^{\infty} \frac{\gamma^{2i}}{(2i)!} \quad (5a)$$

and

$$\frac{\sinh (\gamma)}{\gamma} = \sum_{i=0}^{\infty} \frac{\gamma^{2i}}{(2i+1)!} \quad (5b)$$

With (5a) and (5b), carrying out the Taylor series expansion, all components can be represented in the form of power series:

$$F(s) = \sum_{i=0}^n f_i s^i$$

where  $f_i$  is the coefficient of the expansion.

In order to match the initial condition of the system, the asymptotic frequency point ( $s = j\infty$ ) [12] should be added into the above expansion:

$$F'(s) = F(j\infty) + \sum_{i=0}^n f_i s^i \quad (6)$$

In the above equation, the component steady state response is represented by the moment expansion at  $s = 0$  and the initial condition is satisfied by  $F(j\infty)$ .

To complete the series expansion for each component, we define two types of series operations.

Let

$$A = \sum_{i=0}^n a_i s^i, \quad B = \sum_{i=0}^n b_i s^i$$

where  $Z_0$  is an arbitrary reference impedance, referred to as the characteristic impedance.

The one port element in Figure (1b) has the following S-parameter:

$$S = \frac{Z - Z_0}{Z + Z_0} \quad (2)$$

For an RLC transmission line, we have:

$$S = \frac{1}{2Z_0Z_c \cosh(\gamma) + (Z_c^2 + Z_0^2) \sinh(\gamma)} \begin{bmatrix} (Z_c^2 - Z_0^2) \sinh(\gamma) & 2Z_cZ_0 \\ 2Z_cZ_0 & (Z_c^2 - Z_0^2) \sinh(\gamma) \end{bmatrix} \quad (3)$$

where  $Z_c = \sqrt{\frac{R + sL}{sC}}$  is the characteristic impedance,  $\gamma = \sqrt{(R + sL)sC}l$  is the propagation constant and  $l$  is the length of the line. The derivation of equation (1) through (3) can be found in [1].

The interconnect topology as shown in Figure (1d) can be used to connect components described in Figure (1a) through (1c) to construct a generalized interconnection network. The n-port interconnect node can also be described by the scattering parameter [18]:

$$S = \frac{1}{n} \begin{bmatrix} 2-n & 2 & 2 & \dots & 2 \\ 2 & 2-n & 2 & \dots & 2 \\ 2 & 2 & 2-n & \dots & 2 \\ \dots & \dots & \dots & \dots & \dots \\ 2 & 2 & 2 & \dots & 2-n \end{bmatrix} \quad (4)$$

Combining these four basic elements, one can represent a variety of distributed-lumped network topology including capacitive cutsets, inductive loops, and lossy transmission lines.

Next, the S-parameters defined by equations (1) through (3) are first expanded into Taylor series

## 2. Scattering parameter formulation of distributed-lumped network

Scattering Parameters [1] represent the interrelationship of a set of incoming and outgoing power

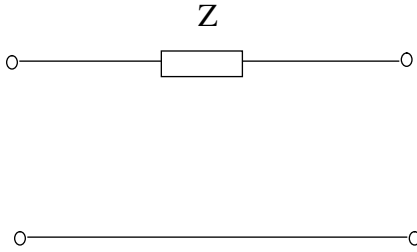


Figure 1a. Two port element.

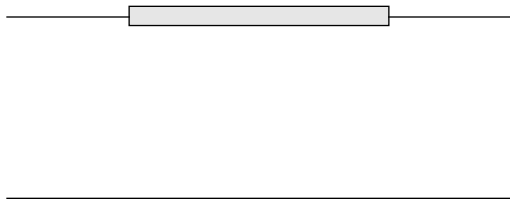


Figure 1c. Lossy transmission line.

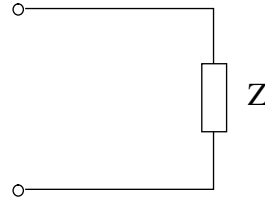


Figure 1b. One port element

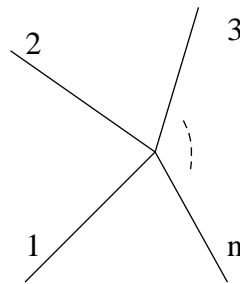


Figure 1d. n-port interconnect node.

waves of a multi-port system. They are frequently used in the microwave field for system description. Some of the advantages of using S-parameters are: (1) they are easier to measure and to work with at high frequencies compare to using other types of parameters, (2) all lumped circuit elements including short and open circuits have unique analytical S-parameter descriptions, and (3) they provide a very convenient means for describing distributed elements such as lossy transmission lines.

To develop the macromodel, we begin with the description of all elements in the distributed-lumped network in terms of their Scattering Parameters. Voltage waves are used for convenience. Four basic elements are utilized to characterize a general interconnect network, namely, 1) shunt (two port) impedance, 2) series (one port) impedance, 3) RLC transmission line and 4) multipoint interconnect node. These basic components are shown in Figures (1a) through (1d).

For a two port element shown in Figure (1a), the S-parameter can be written as:

$$S = \frac{1}{Z + 2Z_0} \begin{bmatrix} Z & 2Z_0 \\ 2Z_0 & Z \end{bmatrix} \quad (1)$$



# S-Parameter Based Macro Model of Distributed-Lumped Networks Using Pade Approximation

## Extended Abstract

### 1. Introduction

Designing of large scale high performance circuits requires precise knowledge of circuit delays. The computation of delays associated with interconnects, in particular, poses a challenging problem and has been the subject of study in current times [2]-[8]. As chip size increases and the length of interconnects become comparable to the wavelength of the signals, the widely accepted RC tree delay model ceases to be adequate and transmission line properties of on-chip and off-chip interconnects gain importance. The Elmore delay based estimation methods, although efficient, are insufficient and the deficiencies of such methods need to be addressed with techniques which are capable of computing delays in the presence of RLC mesh networks, capacitive cutsets, inductive loops, as well as lossy transmission lines.

Recently, an  $n$ -th order extension of Elmore approximation based on Pade moment-matching technique has been developed [9]-[11] to approximate a higher order linear network by the waveforms generated by its lower order moments. The method is referred to as Asymptotic Waveform Evaluation. Several publications have shown the potential of applying Pade approximation for general linear network analysis.

In this paper, we present a Scattering-Parameters (S-Parameters) based macromodel of distributed-lumped networks. One of the many possible applications of the macromodel is delay computation. The networks can include capacitive cutsets, inductive loops, RLC meshes, and lossy transmission lines. An efficient network reduction algorithm is developed and Pade approximation is used to derive the macromodel. In Section 2, we formulate the description of the S-Parameters of the distributed-lumped components. Based on the formulation, in Section 3, we present an efficient network reduction algorithm to reduce the original network into a network containing one multiport component together with the sources and loads of interest. The macromodel is derived in Section 4, and the efficiency and accuracy of the macromodel are well demonstrated, in Section 5, by the transient analysis of several test cases. Finally, Section 6 gives some concluding remarks.